Journal of Natural Products
Vol. 48, No. 5, pp. 689-707, Sep-Oct 1985

APPLICATIONS OF ^{13}C NMR IN THE STUDY OF BIOSYNTHETIC MECHANISM[1]

A. IAN SCOTT

Center for Biological NMR, Department of Chemistry, Texas A&M University, College Station, Texas 77843

ABSTRACT.—Recent applications of high-field nmr spectroscopy in the enzymology of biosynthesis are illustrated. The techniques involve the use of ^{1}H-, ^{3}H-, ^{13}C- and ^{15}N-nmr to focus on individual steps of biochemical processes in the formation of natural products and related enzyme-catalyzed events. In the first set of experiments, pulse labeling studies are used to uncover biosynthetic sequences in the porphyrin-corrin pathway. In the second type of nmr experiment, the application of ^{1}H- and ^{3}H-nmr spectroscopy has illuminated the course of certain key biosynthetic steps in the synthesis of porphyrins and β-lactam antibiotics. These methods have quite general application in biochemical and biological systems. Thirdly, the full magnifying power of the nmr "lens" is used to decipher molecular events during enzyme-catalyzed reactions in solution at subzero temperature and in the solid state.

The study of the biosynthesis of natural products has recently been enriched by the application of high-field nuclear magnetic resonance (nmr) spectroscopy to examine the effects of feeding substrates labeled with stable isotopes in such juxtaposition that the timing of the making and breaking of C-C, C-O, C-N, and C-H bonds during the assembly of a complex product from its constituent building blocks can frequently be reconstructed by post-mortem examination of the target molecule labeled with ^{13}C, ^{18}O, ^{15}N, and ^{2}H. These methods depend on direct observation of isotopic shifts (^{18}O, ^{2}H) on ^{13}C-signals, on C-X spin coupling observation, and, more recently, by spectral editing and two dimensional nmr techniques which, for example, will filter out and edit all ^{13}C-nuclei bound directly to ^{1}H. We now provide examples of some novel nmr techniques designed to probe the biosynthetic pathway at the *single enzyme* level. We first discuss a "hidden" pathway where it can be deduced that several methylating enzymes are at work *in sequence* during the overall transformation of hexa-hydroporphyrin to corrin. Using the nucleus ^{3}H, we next dissect the stages of the actual encounter of the small substrate, porphobilinogen (PBG), with its enzyme (PBG deaminase), an event that initiates the first part of porphyrin (and corrin) synthesis. Turning to a more common (but still mysterious) class of enzyme-catalyzed reaction, we describe both high-field ^{1}H- and ^{13}C-nmr experiments that have been carefully designed to characterize small, labile product molecules released from enzyme and, more importantly, to detect transient *covalent* intermediates bound to enzyme, which are part of the catalytic machinery. The high molecular weights of these productive species (~20,000 MW) require extreme rigor in defining the nmr parameters for their detection. An example from a cognate study of stable transition-state analog inhibitor complexes will be presented. The technique of cross-polarized magic angle spinning is applied to the study of dynamic turnover in solid enzyme-substrate interactions, thus bridging the gap between X-ray diffraction and nmr analysis of biomolecules.

I. BIOSYNTHESIS OF VITAMIN B_{12}: TIMING OF THE METHYLATION STEPS BETWEEN URO'GEN III AND COBYRINIC ACID.—The details of the pathway of corrin biosynthesis beyond the key intermediate uro'gen III (**1**) (1) are still incomplete. The first three enzymatic steps consist of successive C-methylations of uro'gen III at C-2 (2), C-7 (3), and C-20 (4), and the corresponding intermediates have been isolated in their

[1]Presented as a plenary lecture at the "Biologically Active Nitrogen-Containing Natural Products: Structure, Biosynthesis, and Synthesis" Symposium of the International Research Congress on Natural Products at the University of North Carolina, Chapel Hill, North Carolina, July 7-12, 1985.

stable aromatized forms (5), e.g., the 2,7-dimethyl isobacteriochlorin, sirohydrochlorin (**2**) and its 20-methyl derivative, Factor III (**3**). In spite of an intensive search spanning the past ten years (6), the remaining steps are unknown with respect to isolation of intermediates containing four or more methyl groups (up to a possible of eight) but, as noted previously (1), the proven biochemical conversion of Factor III (**3**) to cobyrinic acid (**4**) must involve the following events (see Scheme 1), not necessarily in the order indicated: (a) The successive addition of five methyls derived from S-adenosyl methionine (SAM) to Factor III (**3**); (b) the contraction of the permethylated (seven or eight methyls) macrocycle to corrin; (c) the extrusion of C-20 and its attached methyl group leading to the isolation of acetic acid (7,8,4b); (d) decarboxylation of the acetic acid side-chain in ring C (C-12); and (e) insertion of Co^{2+}. In order to justify the continuation of our search for such intermediates whose inherent lability is predictable, we have applied ^{13}C-pulse-labeling methods to the cell-free system from *Propionibacterium shermanii* (9), which converts uro'gen III (**1**) (1,9) and sirohydrochlorin (**2**) (3,10) to cobyrinic acid (**4**), a technique used previously in our laboratory to detect the flux of ^{14}C-label through the intermediates of alkaloid biosynthesis in higher plants (11).

It was argued that the full methylation cascade could be differentiated in time, provided that enzyme-free intermediates accumulated in sufficient pool sizes to affect the resultant methyl signals in the ^{13}C-nmr spectrum of the target molecule, cobyrinic acid (**4**), when the cell-free system is challenged with a pulse of $^{12}CH_3$-SAM followed by a second pulse of $^{13}CH_3$-SAM (or vice versa) at carefully chosen intervals in the total incubation time (9-10 h). By this approach, it should be possible to "read" the biochemical history of the methylation sequences as reflected in the dilution (or enhancement in the reverse experiment) of $^{13}CH_3$-label in the seven methionine-derived methyl groups of cobyrinic acid after conversion to cobester (**5**), whose ^{13}C-nmr spectrum has been completely assigned (1,12,13).

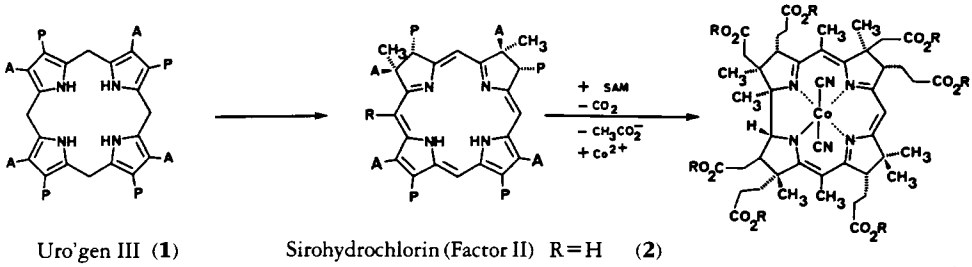

Uro'gen III (**1**)

Sirohydrochlorin (Factor II) R=H (**2**)
Factor III R=CH_3 (**3**)

Cobyrinic acid R=H (**4**)
Cobester R=CH_3 (**5**)

SCHEME 1

The validity of the method was tested in a preliminary experiment using a two-phase system. $^{13}CH_3$-Methionine (90% ^{13}C; 30 mg) was added to a whole-cell (100 g) suspension of *P. shermanii* in phosphate buffer containing δ-aminolevulinic acid (20 mg), in the absence of Co^{2+}. Under these conditions, the cells produce uro'gen III (**1**), sirohydrochlorin (**2**), and Factor III (**3**), but no corrin. Cell disruption and incubation of the extract (10) with added Co^{2+} and pulses of $^{12}CH_2$-SAM at varied intervals was monitored for differential methylation by isolation of cobyrinic acid, conversion to cobester (**5**), extensive purification and, finally, ^{13}C-nmr analysis of the enriched samples (normally 50-150 μg). Optimization of these conditions led to the spectrum shown in Figure 1, which reveals a clear distinction between the peak heights of the seven methyl groups of cobester when compared with a spectrum obtained by adding $^{13}CH_3$-SAM at the outset. The high relative intensities of the C-2 and C-7 signals bear testimony to the initial formation in whole cells of the 2,7-dimethyl isobacteriochlorin,

sirohydrochlorin (**2**), in the absence of Co^{2+}. The differential dilution of methyl intensity in cobester not only suggests that free intermediates have accumulated, but that even in this qualitative experimnent, the sequence of methylation is revealed at C-2 ≈ C-7>C-17>C-12α>C-1>C-5 ≈C-15, since the timing of the addition of $^{12}CH_3$-SAM dilutes the pool sizes of $^{13}CH_3$-enriched methylated intermediates in the order in which they are formed. Thus, C-17 is the site of the fourth, C-12α the fifth, and C-1 the sixth methylation. Note that the experiment does not distinguish C-5 from C-15 (the seventh and eighth methylations) (14).

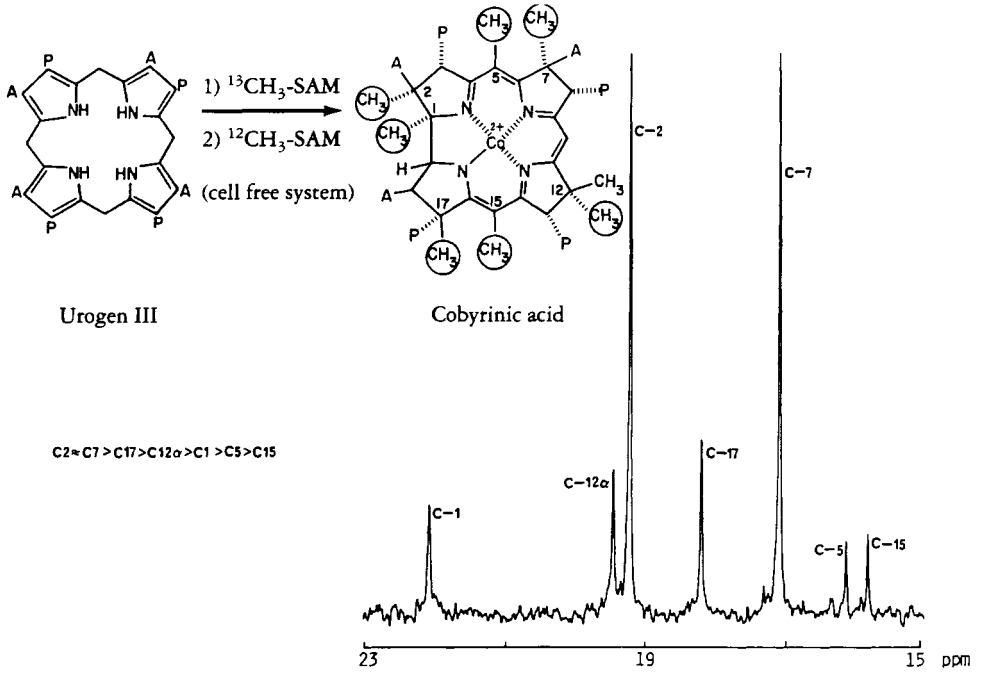

FIGURE 1. 125 MHz, broad band, ^{1}H-decoupled (1 w), ^{13}C-nmr spectrum of ^{13}C-enriched cobester (**5**) (270 μg in 0.5 ml KCN saturated benzene-d_6) isolated from *P. shermanii* (see text for incubation details). Chemical shifts are with respect to tetramethylsilane (TMS) at 0 ppm. Spectral parameters: spectral width, 30 ppm; pulse repetition rate, 0.7 sec; α, 65°. Spectrum represents the sum of 51,382 free-induction decays (FIDs) with 2.0 Hz line broadening.

Finer tuning of the experiment was achieved in the reversed pulse mode using a porphyrin-free, cell-free system and unlabeled sirohydrochlorin (900 μg) (**2**) as substrate. Incubation with $^{12}CH_3$-SAM was followed by a pulse of $^{13}CH_3$-SAM (15) after an interval (ca. 6 h), which allowed the accumulation of unlabeled intermediates. The resultant cobester (**5**) will bear only five enriched methyls, at C-1, C-5, C-12α, C-15, and C-17. The spectrum shown in Figure 2a provides striking confirmation and extension of the preliminary experiment in that the relative intensities of C-12α and C-17 are much lower than that of C-1, which, in turn, is differentiated from C-5 and C-15 (14), i.e., the pulse of $^{13}CH_3$-SAM is diluted by an accumulated pool of unlabeled tetra- and penta-methyl intermediates and becomes available for more efficient labeling of the hexa-⟼octa-methyl intermediates. Control experiments show that early pulsing (0-60 min) leads to a spectrum of cobester showing approximately equal intensity of all five methyls after "normalization" for C-5 and C-15 (14) (Figure 2b), while late addition (~9 h) affords unlabeled cobester. Thus, the complete sequence of methylation of uro'gen III can be described as C-2>C-7>C-20>C-17>C-12α>C-1>C-5≈ C-15, a result which complements and extends a report on the differentiation of C-17 as the fourth methylation site in a pulse experiment with extracts of a different bacterium,

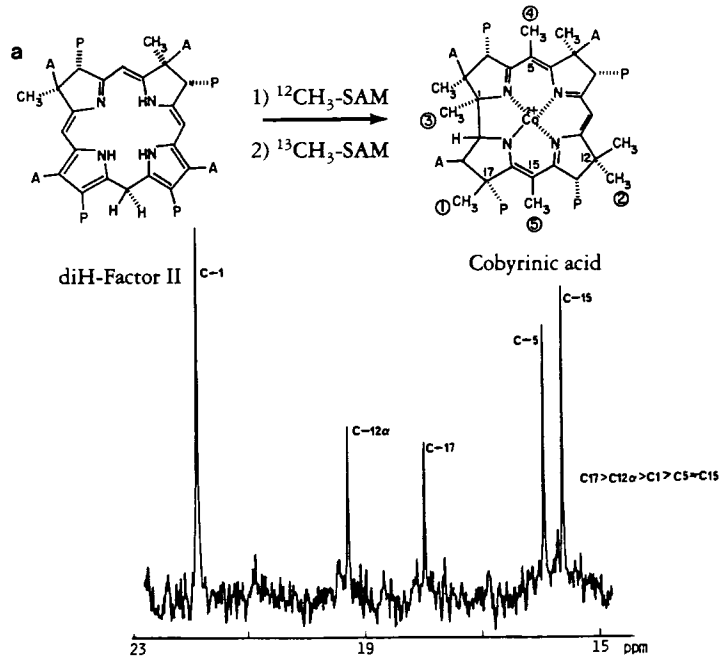

FIGURE 2a. Spectrum of enriched cobester (**5**) (46 g), accumulated as in Figure 1, with 112,340 FIDs. See text for incubation conditions.

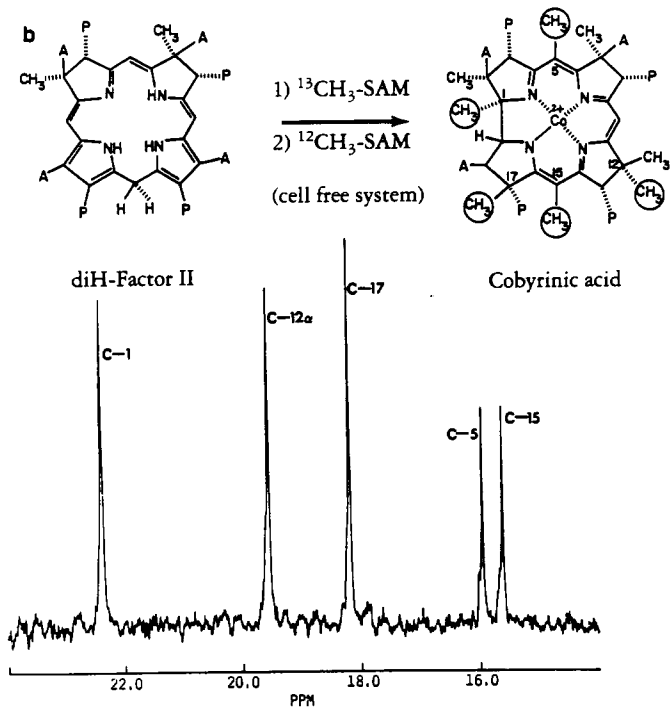

FIGURE 2b. Spectrum of enriched cobester (**5**) (105 μg), accumulated as in Figure 1, with 79,080 FIDs. See text for incubation conditions.

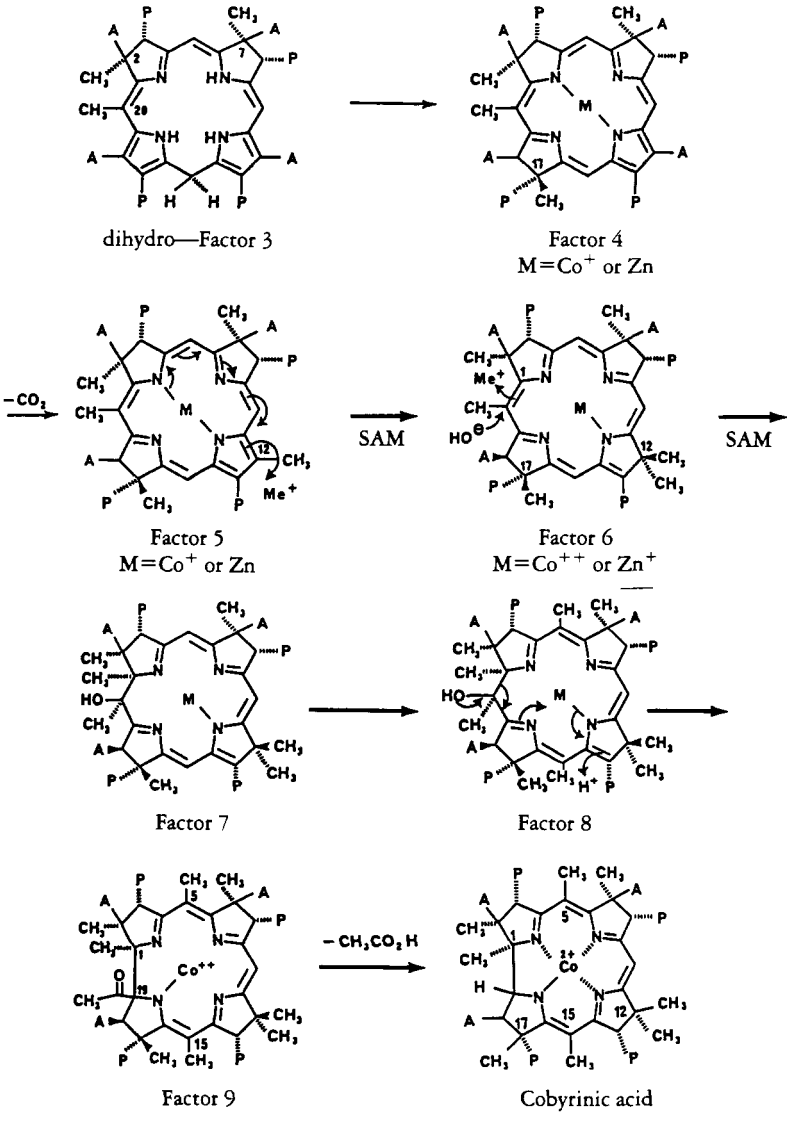

SCHEME 2

Clostridium tetanomorphum (16). On the basis of this sequence, we propose the structures shown in Scheme 2 as the targets of the search for the "missing" intermediates of corrin biosynthesis. For example, the pyrrocorphin structures suggested for Factors 5 and 6 take into account the sequence C-17 methylation, decarboxylation of the C-12 acetate side-chain, and C-12α methylation. Similarly, the structures of Factors 7 and 8 are proposed to rationalize the methylation of C-1 and the hydration of C-20 as a prelude to the ring contraction/acetic acid extrusion (↦Factor 9) for which we have used Eschenmoser's in vitro analogy (17). The final methyl functionalizations at C-5 and C-15 (in Factor 9) are suggested to *follow* Co^{2+} insertion (1,18,19), since hydrogeno cobyrinic acid is *not* involved in corrin biosynthesis (20). A metal complex template—not necessarily CO^{+++}—may stabilize Factors 4-9. For example, zinc corphinate or pyrrocorphinate structures can be promulgated for Factors 4-8, where M=Zn or Zn^+, and the loss of acetic acid may well take place from the *cobalt* complex of Factor 9 based on the work of Nussbaum and Arigoni (21). These later steps, however, can only be defined

when the intermediates have been discovered. However, the most important implications of the differential incorporations of SAM-derived methyl groups into cobester as a function of time are as follows:

(a) Several stable enzyme-free intermediates must accumulate.

(b) There appear to be *at least* five "methylases" responsible for the uro'gen-corrin connection. Methylase I (C-2, C-7), which has already been shown (10) to transform uro'gen III as far as the mono- and di-methyl intermediates Factors I and II (**2**), methylase II (C-20), methylase III (C-17), methylase IV (C-12), and methylase V (C-1, C-5, C-15).

(c) The fact that cobalt-deficient cells produce substantial amounts of C-2, C-7, and C-20 methylated intermediates (as **2** and **3**) but insufficient tetra-↦octa-methyl intermediates to perturb the ratio of methyl labeling in cobester (Figure 1) suggests that similar pulse experiments with Co^{2+} should define the point at which cobalt insertion takes place.

In summary, the experiments described above (22) suggest that the search for compounds related to the structures suggested in Scheme 2 can now proceed with confidence.

Further refinement of the experiment in which the incubation was pulsed with $^{13}CH_3$-SAM after an interval of only 3-4 h afforded a spectrum of cobester (**5**) in which the signal C-17 had almost disappeared, leading to complete differentiation between the methylation times for C-17 (3-4 h) and C-12α (4-6 h) (Figure 3). This implies that discrete methylating enzymes are involved at these two centers and at C-2/7, C-20, C-1, and C-5/15 (22), and that, finally, the possibility of isolating the missing factors, perhaps as their complexes with metals other than cobalt, can become a reality.

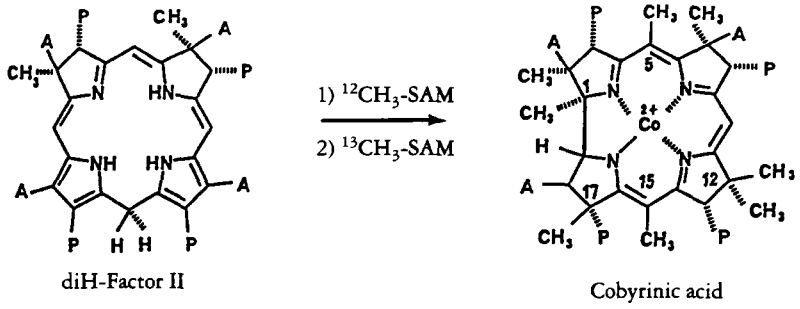

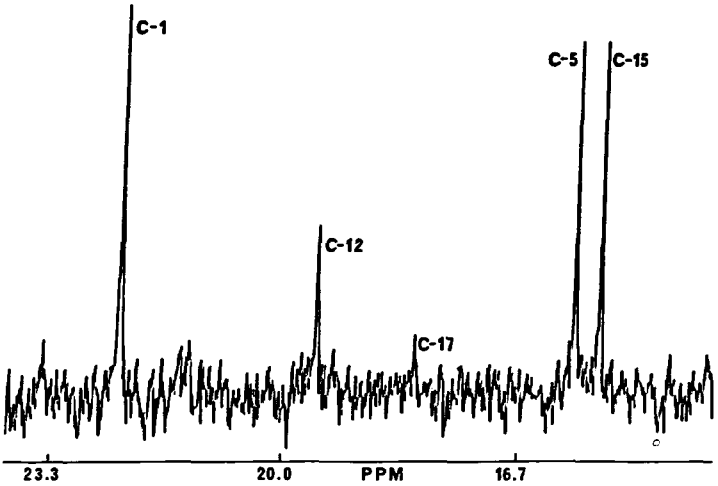

FIGURE 3. Spectrum of enriched cobester (**5**) (50 μg), accumulated as in Figure 1. See text for incubation conditions.

II. DIRECT OBSERVATION OF ENZYME-SUBSTRATE COMPLEXES BY TRITIUM Nmr SPECTROSCOPY.—The central role of uro'gen III (**1**) in heme, chlorophyll, and corrin biosynthesis has captured and maintained the interest of bioorganic chemists in the mechanism of action of the two enzymes required for the synthesis of **1** from porphobilinogen (PBG, **6**). We now describe recent nmr experiments with the first of these enzymes, PBG deaminase (EC 4.3.1.8), which catalyzes the head-to-tail condensation of 4 mol of PBG (**6**) to pre-uro'gen, whose release and stabilization as the (hydroxymethyl)bilane (HMB, **12**) has been the subject of extensive investigation (23-26). HMB may cyclize chemically to uro'gen I (**13**) or serve as the substrate for uro'gen III cosynthetase (EC 4.2.1.75) to form uro'gen III (**1**) (Scheme 3).

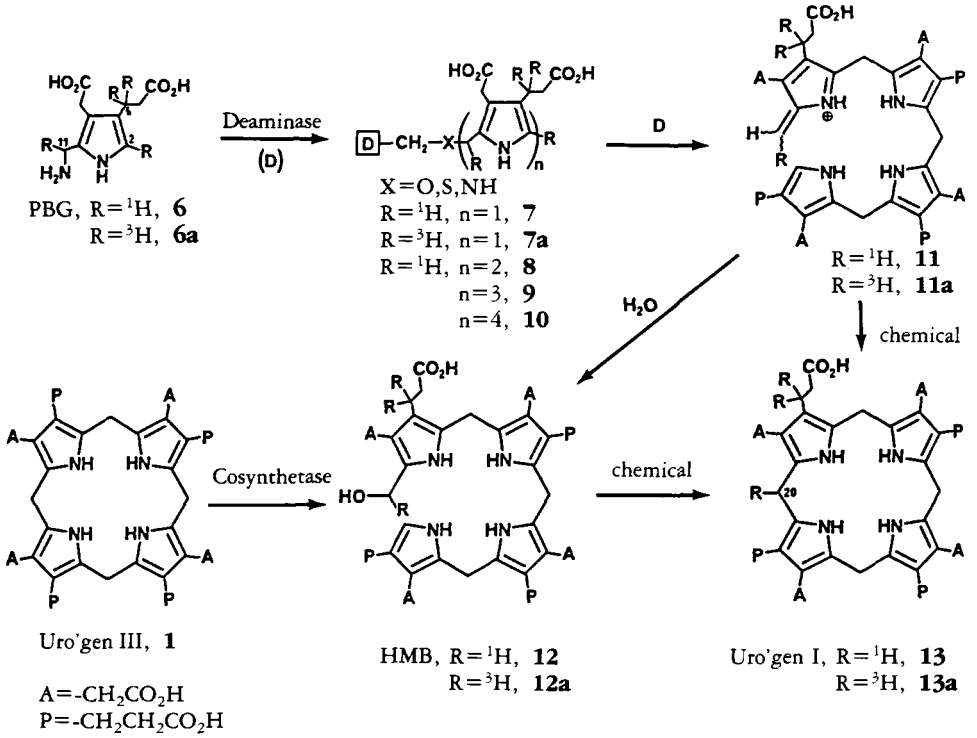

SCHEME 3

Deaminase (MW~36,000) from human sources (27), *Rhodopseudomonas spheroides* (28-30), and *Euglena gracilis* (31,32) forms stable covalent complexes bearing up to four condensed PBG units. It has been suggested (27-32) that the amine function at C-11 of PBG is replaced by a nucleophilic "X" group at the active site of deaminase, where X=O, S, or NH to form **7-10** (Scheme 3). The introduction of ^{13}C enrichment at C-11 should allow observation of the chemical shift for the new CH_2X group in the region 25-60 ppm. In our hands, experiments using [2,11-$^{13}C_2$]PBG to label the complexes **7-10** provided no ^{13}C-nmr evidence for enrichment above natural abundance either in the above complexes or in the proteolytic digests of the mono-PBG complex (27,28,33) due to the combination of large line widths and high density of resonances in the region of interest. This result contrasts with a recent claim (32) for ^{13}C-signal enhancement near 42 ppm, consistent with amine functionality at the active site (**7**, X=NH). In view of the high natural abundance profile near 40 ppm in the ^{13}C-spectrum of deaminase (32,33) and the resultant ambiguity of assignment in the CH_2X region, we sought a general solution to structural problems in covalent enzyme-substrate complexes where the lack of a "window region" precludes rigorous assignment and now des-

cribe the first application of tritium, a nucleus of high sensitivity and low ($<10^{-16}$) natural abundance (34), as an nmr probe of chemical shift in the environment of a productive covalent complex of enzyme and substrate.

[2,6,6,11,11-$^3H_5$]PBG (**6a**) (35) (132 Ci/mmol) was synthesized from [3,3,5,5-$^3H_4$]-5-aminolevulinic acid (ALA) (36) by the action of ALA dehydratase from *R. spheroides* (37). The ^{1}H-decoupled ^{3}H-nmr spectrum of **6a** (Figure 4i) confirmed the position of ^{3}H-labeling by comparison with the ^{1}H-nmr spectrum of PBG. The resonances occur at 6.69 (C-2, CT), 4.15 (C-11, HCT), 2.62 (C-6, HCT), and 2.56 ppm (C-6, CT_2). The tritiated PBG was rapidly mixed with highly purified (>95%) deaminase (38) [4000 units (39)] from *R. spheroides* and the covalent complexes separated from small molecules by gel filtration on G-50 Sephadex. Analysis of the concentrate by analytical gel electrophoresis showed it to be >90% of the monopyrrole complex (27,28) (**7a**; 16 mCi). The ^{3}H-spectrum (Figure 4ii) of **7a** exhibits resonances (40) at 6.18 (C-2, CT), 3.28±0.1 (pyrrole-CHT-X-Enz), and 2.48±0.1 ppm (pyrrole-$CT_2CH_2CO_2H$) at 5.5°C. At 23° (Figure 4iii) the signals at 6.18 and 3.28 ppm disappear and are replaced by new resonances at 3.58±0.1 [meso methylenes (CHT) of uro'gen I (**13a**) and methylenes (CHT) of complexes **8-10**, R=^{3}H], 2.75±0.1 ($CT_2CH_2CO_2H$ of **8-10**, R=^{3}H), 2.48±0.1 [$CT_2CH_2CO_2H$ of uro'gen I (**13a**)], and 4.69 ppm (HOT, exchanged from C-2—also present in Figure 4, spectra ii and iv). The formation of uro'gen I (**13**) (whose ^{3}H-chemical shifts are identical with the corresponding CH_2 resonances in the ^{1}H-nmr spectrum) in absence of free PBG is ascribed to disproportionation of complex **7a** via **8-10** whose methylene (CHT) and side-chain groups (C-$T_2CH_2CO_2H$) can be observed along with those of uro'gen I in the signals at 3.58, 2.75, and 2.48 ppm. Such a disproportionation also accounts for the disappearance of the signal at 3.28 ppm, which would be expected to lose up to 90% of its origi-

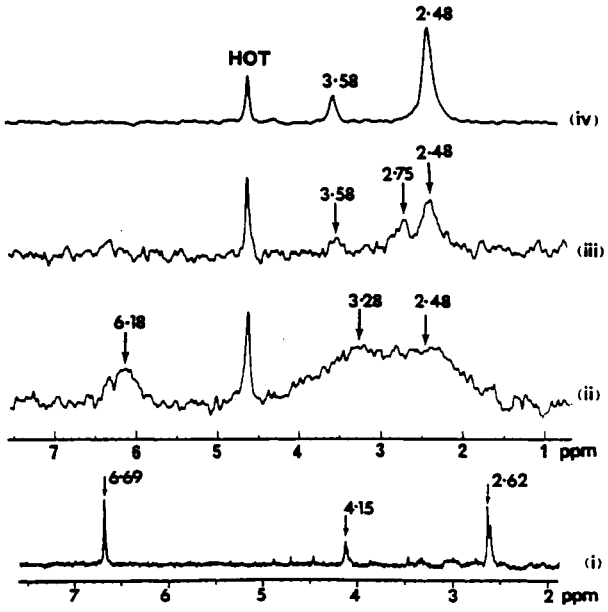

FIGURE 4. (i) ^{1}H-decoupled 320 MHz ^{3}H-nmr spectrum of [2,6,6,11,11-$^3H_5$]PBG at pH 8.0, 25°. (ii) ^{1}H-decoupled 320 MHz ^{3}H-nmr spectrum of [2,6,6,11,11-$^3H_5$]PBG deaminase complex at pH 8.0, 5.5°. (iii) Same as (ii) but at 23°. (iv) Same as (ii) plus unlabeled PBG (950 μg) and after 40 min at 3.5° and 6 h at 23°.

nal intensity, on the basis of the statistical randomization of ^{3}H-label, from **7a**→**8**→**9**→**10**→**13**.

To demonstrate the catalytic competence of the monopyrrole complex **7**, *unlabeled* PBG (**6**) was added to the ^{3}H-complex **7a** at 3.5° and the formation of uro'gen I monitored by ^{3}H-nmr. At 3.5°, a transient low-intensity signal was observed at 4.76 ppm, a chemical shift consistent with the vinyl (R) hydrogen of the azafulvene (**11a**) (41). On warming to 23° (Figure 4iv), sharp resonances for unbound uro'gen I (**13a**) appeared at 3.58 (20-meso CHT) and 2.48 ppm (propionate CHT) corresponding to the ^{1}H-chemical shifts in an enzyme-free sample of uro'gen I (38).

The large line widths of the spectrum in Figure 4 (spectra ii and iii) (~150-300 Hz) reflect an environment in which the active site of the enzyme is probably buried within the protein. The line width of the propionate side chain also suggests that it is covalently attached or ionically associated with the protein, which is consistent with literature reports on the inhibitory effects of PBG analogues (42-46). The ^{3}H-chemical shift (3.28±0.1 ppm) of the methylene directly attached to the enzyme allows conclusions to be drawn as to the nature of the nucleophilic group "X" in Scheme 3. That the methylene could be bound to the oxygen of a serine residue is ruled out, inasmuch as HMB (**12**) and its methyl ether have chemical shifts of 4.4 and 4.2 ppm, respectively (38). Model studies (47) predict δ 3.9 for methylene attached to amine, while the observed value (3.28±0.1 ppm) is more consistent (49) with a thioether linkage (**7a**, X=S). We therefore suggest that the active-site nucleophilic group in deaminase is a cysteine thiol residue or, less probably, an amino group (**7a**, X=NH), which, on covalent binding to C-11 of PBG, leads to an upfield shift of ~0.6 ppm from the anticipated value of 3.9 ppm. The former possibility is supported by the observation that deaminase is reversibly inhibited by sulfhydryl blocking reagents (50).

The example of deaminase discussed above (51) represents a specific and unique case of stabilization of a productive intermediate due to insufficiency of substrate. We now discuss the more general and technically more difficult problem of studying enzyme *mechanism* by direct nmr methods.

III. STUDYING ENZYME MECHANISM BY ^{13}C-nmr.—Almost all enzymatic processes utilize multistep reactions during catalysis, and the characterization of each of these stages is essential if one is to understand enzyme mechanism at the molecular level. Earlier investigators have used spectrophotometric methods for characterizing enzyme-catalyzed reactions, whereas inhibitors that form stable "transition state analogues" have been examined by other techniques that require long periods of data accumulation, for example, X-ray analysis. However, the advent of nmr and its subsequent use in enzymology are beginning to provide a novel and penetrating probe for elucidating enzyme mechanism by directly characterizing intermediates formed in catalysis. The studies of "transition state analogues" allow access to the unique properties of enzymes that enable them to stabilize labile intermediates and therefore achieve their remarkable catalytic efficiency. We discuss first the structures of an enzyme-inhibitor adduct of the serine protease, trypsin, and compare the results of direct observation by ^{13}C-nmr with the structural information inferred by more classical techniques. We then review the powerful combination of nmr and cryoenzymology. The development of this technique, whereby enzyme-catalyzed reactions are studied at subzero temperatures in aqueous organic solvents (cryosolvents), allows such reactions to be slowed down and can prolong the lifetime of enzyme-substrate intermediates (52).

Scheme 4 shows the generally accepted mechanism for the hydrolysis of an amide function by a serine protease and is representative of the mechanism for all the hydrolyses. To confirm this mechanistic pathway, the visualization and rigorous characterization of productive tetrahedral intermediates and acyl enzymes by ^{13}C-nmr is the ulti-

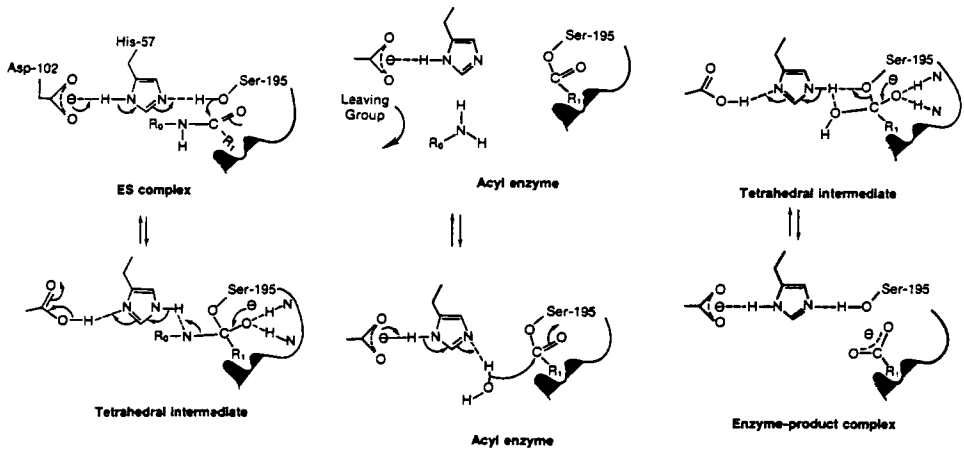

SCHEME 4

mate goal, and we now discuss the progress made so far, particularly with the serine and thiol proteases.

In the domain of synthetic inhibitors, chloromethylketone derivatives of specific substrates are potent irreversible covalent inhibitors of the serine proteases, alkylating the active-center histidine at N-2 (see Scheme 4). X-ray crystallographic studies (53) led to the suggestion that, in addition to the above alkylation, there was also nucleophilic attack by the active-center serine hydroxyl to form a hemiketal, which is stereochemically analogous to the tetrahedral intermediate purported to occur during catalysis.

To test this suggestion, trypsin was inhibited with the highly specific reagent N^{α}-carbobenzyloxylsylchloromethylketone (54) ($RCOCH_2Cl$), labeled in the ketone carbon with 90% ^{13}C, for it was predicted that a tetrahedral adduct, if formed, would be directly observable by this technique. In aqueous solution (Figure 5a), $RCOCH_2Cl$ exists as a mixture of the ketone ($\delta=204.7$ ppm) and its hydrate ($\delta=95.4$ ppm). At pH 3.2 no alkylation or inhibition of the enzyme is observed and the spectrum of $[^{13}C{=}O]RCOCH_2Cl$ is unperturbed (Figure 5, b and c), showing that at low pH there is no detectable binding or tetrahedral adduct formation prior to alkylation. At pH 6.9 there is rapid, irreversible inhibition, and resonances due to both $[^{13}C{=}O]RCOCH_2Cl$ and its hydrate are replaced by a single resonance at 98.0 ppm (Figure 5d), an indication that the ^{13}C-enriched carbonyl of the inhibitor is tetrahedrally coordinated in the inhibitor-enzyme adduct. Denaturation of the trypsin led to reappearance of a carbonyl resonance (205.5 ppm) and a decrease in the intensity of the resonance at 98.0 ppm. This demonstrates that the tetrahedral adduct formed by the attack of the serine hydroxyl on the inhibitor carbonyl and characterized by the resonance at 98.0 ppm requires an intact trypsin structure (55).

In the above experiments with $[^{13}C{=}O]RCOCH_2Cl$ and trypsin, it is difficult to discount the possibility that the resonance at 98.0 ppm could result from hydration of the carbonyl of the covalently bound inhibitor. However, the use of ^{18}O isotopic shifts on the ^{13}C spectrum of the tetrahedral adduct has now shown the adduct is indeed formed by nucleophilic attack of the Ser^{195} hydroxyl group (56).

IV. THE QUEST FOR TRUE INTERMEDIATE STRUCTURE: CRYOENZYMOLOGY.—The detection and characterization of a productive acyl intermediate by ^{13}C-nmr during catalysis with natural substrates at ambient temperatures is not possible at present, because there is an inherent lack of sensitivity in ^{13}C-nmr spectroscopy. There-

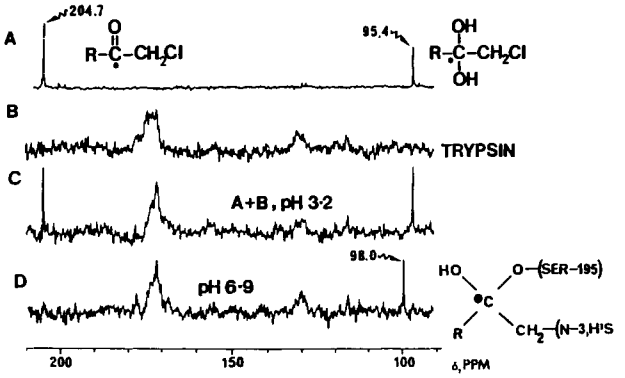

FIGURE 5. The ^{13}C-nmr spectra of (a) N^{α}-carbobenzyloxylsyl-chloromethylketone ($RCOCH_2Cl$); ●=^{13}C, 90% enrichment; 47.6 mM (by weight); 1 mM HCl; D_2O, 16.7% (by volume); volume, 0.6 ml; 1660 accumulations; pH 3.1; (B-D) 20 mM sodium phosphate; 12.5% (by volume) D_2O; 10,000 accumulations; trypsin, 0.28 mM (concentration of fully active enzyme); volume, 8 ml. The $RCOCH_2Cl$ concentrations, pH and enzyme activities were as follows: (b) 0.00 mM, 3.2, 100%; (c) 0.38 mM, 3.2, 100%; (d) 0.37 mM, 6.9, 0.06%. All spectra were accumulated on a Bruker WM300 WB spectrometer at 75.4 MHz for ^{13}C nuclei.

fore, the lifetimes of these intermediates must be extended into the domain of the nmr experiment. One approach is to use synthetic substrate analogues that deacylate slowly. Another is to utilize low-temperature cryoenzymological techniques to extend the lifetimes of intermediates.

Because the ^{13}C resonances of the carbonyl carbon of thioesters are shifted (Δ 20 to 30 ppm) upfield relative to their oxygen analogues ($\delta \approx$ 165 to 185 ppm), ^{13}C-nmr spectroscopy should allow the direct monitoring of the formation and decay of a thioacyl intermediate. Using [^{13}C=O]*N*-benzoylimidazole (δ=168.7 ppm), we were able to observe directly a thioacyl intermediate at δ=195.9 ppm in the presence of papain under the cryoenzymological conditions of $-6°$ in 25% aqueous dimethyl sulfoxide (57) (Figure 6). Moreover, the thioacyl species is clearly a productive intermediate since the decrease in its signal intensity was accompanied by an increase in the product resonance and by release of free enzyme (half-life, $\approx$ 96 min) determined by titration of its thiol group. The line width of the resonance at 195.9 ppm was 25±5 Hz.

The trypsin-catalyzed hydrolysis (Figure 7) of the highly specific substrate N^{α}-carbobenzyloxy-L-lysine-*p*-nitrophenylester (*Z*-lys-pNP) has been studied in detail under cryoenzymological conditions by both spectrophotometry (58) and ^{13}C-nmr spectroscopy (59). The kinetic data from both techniques confirm that the kinetics and mechanism under cryoenzymological conditions are essentially the same as those determined at ambient temperatures by rapid reaction techniques. The hydrolysis of [l-^{13}C]*Z*-lys-pNP (S in Figure 7a, δ=173.6 ppm) by trypsin was monitored by the decrease in intensity of this signal and the increase in the signal arising from the product (P_2 in Figure 7a, δ=177.7 ppm) at $-21°$ in 41% aqueous dimethyl sulfoxide (Figure 7). The continued formation of product (P_2) after all the substrate has been consumed (Figure 7b) provides indirect evidence for an enzyme-bound intermediate whose line width is much greater than that of the free substrate or product and is therefore not di-

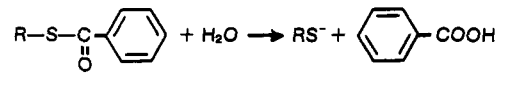

RSH=Papain

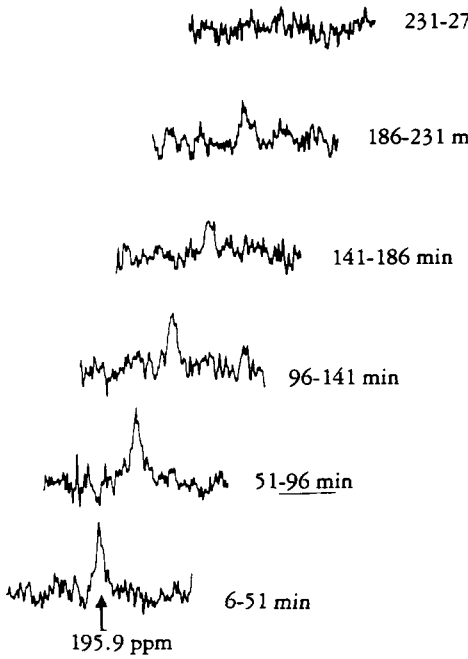

FIGURE 6.

Reaction of 1.7 mM papain (72% active enzyme), 5.4 mM KCl, 25% (by volume) DMSO, 0.1 M sodium formate buffer (pH 4.1), and 23.6 mM benzoylimidazole. [^{13}C=O]Benzoylimidazole was added at 0°; after 15 min the reaction was cooled to −6°, and the nmr data acquisition commenced 6 min after the reaction was initiated. Spectra represent 10,000 accumulations recorded sequentially starting 6, 51, 96, 141, 186, and 231 min after adding benzoylimidazole (57). The spectral range shown is 192 to 200 ppm.

rectly observable in the individual ^{13}C-nmr spectra of Figure 7. Improvement of the signal-to-noise ratio by summation of sets of the individual spectra in Figure 7 made it possible to use difference techniques and allowed direct observation (Figure 8b) at −21° of a resonance (δ=176.5 ppm) that was assignable to the acyl enzyme on the basis of its chemical shift and the kinetics of its breakdown-formation. Experiments at −1.5° (Figure 8a) showed that the acyl intermediate was much more readily detected at this

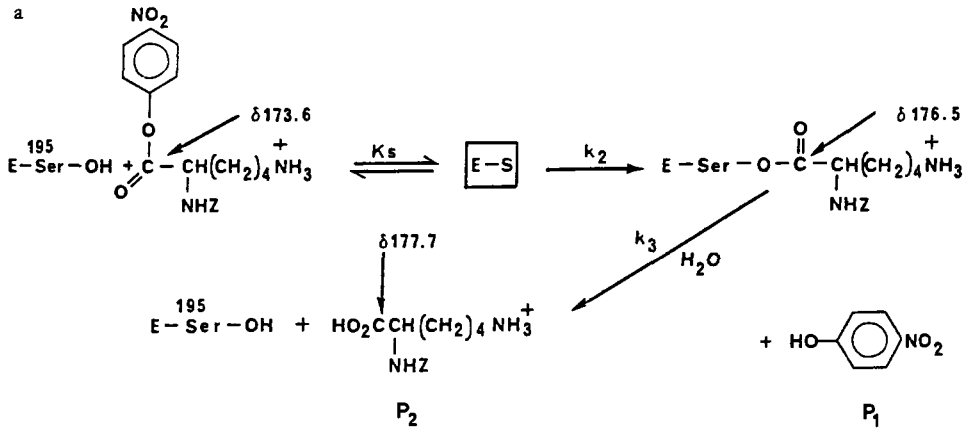

FIGURE 7a. Reaction of [1-^{13}C]Z-lys-pNP, 0.83 mM; active trypsin, 0.7 mM; 1 mM HCl (apparent pH, 3.2); and 40% (by volume) DMSO (sample volume, 10 ml; sample temperature, −21°); NHZ, carbobenzyloxy-. The reaction was initiated by the addition of [1-^{13}C]Z-lys-pNP; after mixing ($\approx$1 min) nmr data acquisition.

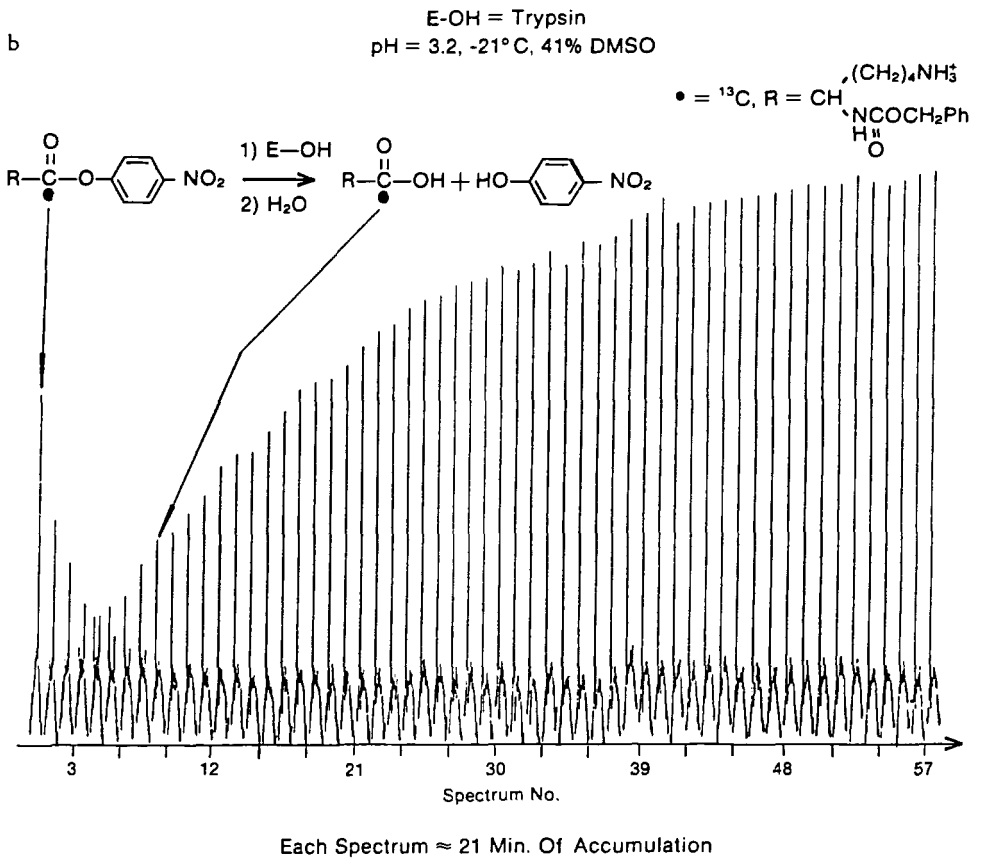

FIGURE 7b. Commenced within 3 min. Each spectrum (1 to 58) represents 10,000 accumulations (time per spectrum, 41 min) recorded sequentially (59). The spectral width was 0 to 220 ppm, but only the region from 172 to 180 is shown.

higher temperature, the resonance being clearly resolved in individual spectra as a result of the smaller line width of the resonance at $-1.5°$ compared to that at $-21°$ (22 ± 3 Hz and 100 ± 10 Hz, respectively). This illustrates one of the main difficulties of a combined nmr-cryoenzymological approach in which the line width of enzyme-bound species increases dramatically as the cryosolvent viscosity increases on lowering the temperature.

V. SOLID-STATE nmr AS A PROBE FOR ENZYME-SUBSTRATE STRUCTURE.—The basis for all of the nmr studies with proteases has relied heavily on the crystal structure determination of the enzyme and/or enzyme complex at the active site (60). Inasmuch as the phase change from solid to solution may well involve considerable conformational alteration, the correlation of the two physical methods (X-ray, nmr) in the same phase would be a desirable objective in furthering our understanding of enzyme mechanism. Our final theme concerns the application of solid-state, cross-polarized magic angle spinning (cpmas) nmr spectroscopy to the direct observation of the hydrolysis of a slow (pseudo) substrate catalyzed by an enzyme. Magic angle spinning (mas) nmr has already been shown to be a powerful technique for the study of solids generally (61) and has been used extensively on inorganic systems (62).

The crystal structures of several complexes of the metalloenzyme, carboxypeptidase Aα (CPA) (EC 3.4.17.1), have been examined in considerable detail. The structure of the complex with glycyl tyrosine (Gly-Tyr) has been refined to 2.0 Å resolution (63,64)

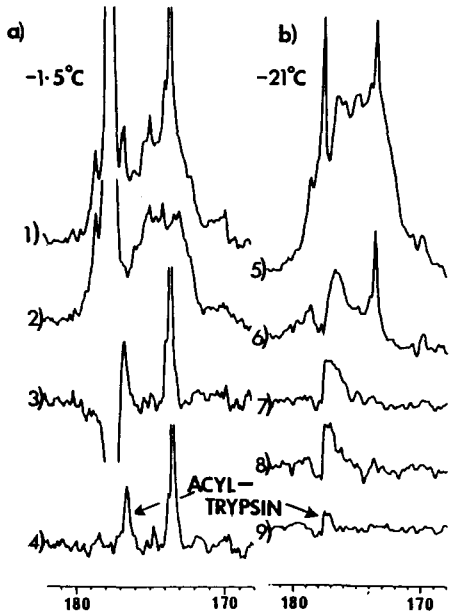

FIGURE 8. The ^{13}C-nmr spectra of the reaction of (a) [1-^{13}C]Z-lys-pNP, 1.8 mM; active trypsin, 0.64 mM; 1 mM HCl (apparent pH, 3.02); and 40% (by volume) DMSO (sample volume, 10 ml; sample temperature, −1.5°). The reaction was initiated as described in Figure 7, and spectra 1 to 15 (not shown) were recorded sequentially in the manner of Figure 7b. Each spectrum resulted from 5000 accumulations (time per spectrum, 20.5 min). A 10 Hz exponential weighting factor was used. Spectra 1 and 2 represent the sums (25,000 accumulations of spectra 1 to 5 and spectra 11 to 15, respectively). Spectrum 3 is the difference between spectra 1 and 2. Spectrum 4 is spectrum 1 from which natural abundance trypsin and product have been subtracted. (b) The free induction decay spectra from which the spectra in Figure 7b were obtained were added together in groups of ten. Spectrum 5 represents the sum of spectra 2 to 11 (of Figure 7b). Spectra 6 to 9 represent progressive subtractions of added spectra 12 to 21, 22 to 31, 32 to 41, and 49 to 58 from which product and natural abundance trypsin resonances had been subtracted.

and reveals, among other things, interactions between the amide carbonyl oxygen and the catalytically essential zinc, and between the amide nitrogen and the hydroxyl of tyrosine-248 (Tyr-248) (Figure 9a). The proposed mechanisms for hydrolysis of peptide and ester bonds by CPA have relied heavily on these crystal structures, but a clear distinction between the possible roles of glutamate-270 (Glu-270) in nucleophilic attack either by general base catalysis (Figure 9a) or by covalent anhydride formation (Figure

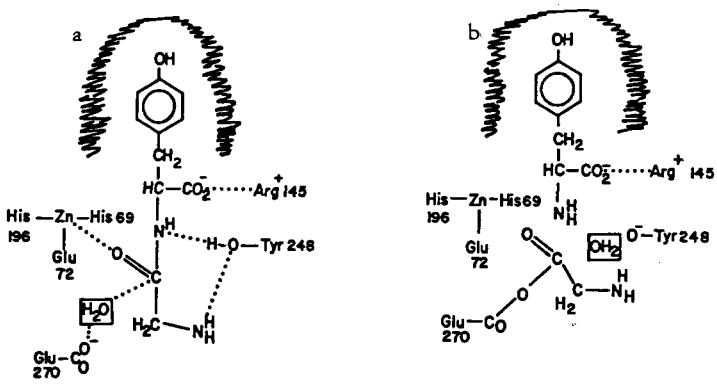

FIGURE 9. (a) Represents Gly-Tyr bound to CPA showing the indirect attack of Glu-270 promoting the attack of a water molecule on the substrate's amido carbonyl group polarized by interaction with zinc. (b) Represents direct attack of Glu-270 on the substrate's amido carbonyl forming an anhydride.

9b) remains a major unresolved problem. Indeed, it is not yet certain whether esters and amides are hydrolyzed by CPA via identical mechanisms (65).

Gly-Tyr was synthesized as both the [^{13}C]-amido (90 atom % enrichment) and amido-[^{13}C, ^{15}N] (90 atom % and 99 atom % enrichment, respectively) isotopomers by known methods (66). CPA, purchased from Sigma as a suspension in toluene, was crosslinked (67) and soaked with Gly-Tyr as described previously (63) and the washed, dried crystals examined by solid-state nmr. The ^{13}C cpmas nmr spectrum of the ^{13}C-enriched Gly-Tyr (Figure 10a) displays residual (68) ^{13}C-^{14}N quadrupolar coupling ($\delta = 176$ ppm]. However, the ^{13}C cpmas difference spectrum of CPA and the CPA/Gly-Tyr complex (Figure 10b) displays a *single resonance* (δ 178 ppm, LW½ 60 Hz) revealing that, under the experimental conditions, the peptide bond of this slow-reacting substrate has been cleaved to the extent of >90%. In order to confirm this result, doubly

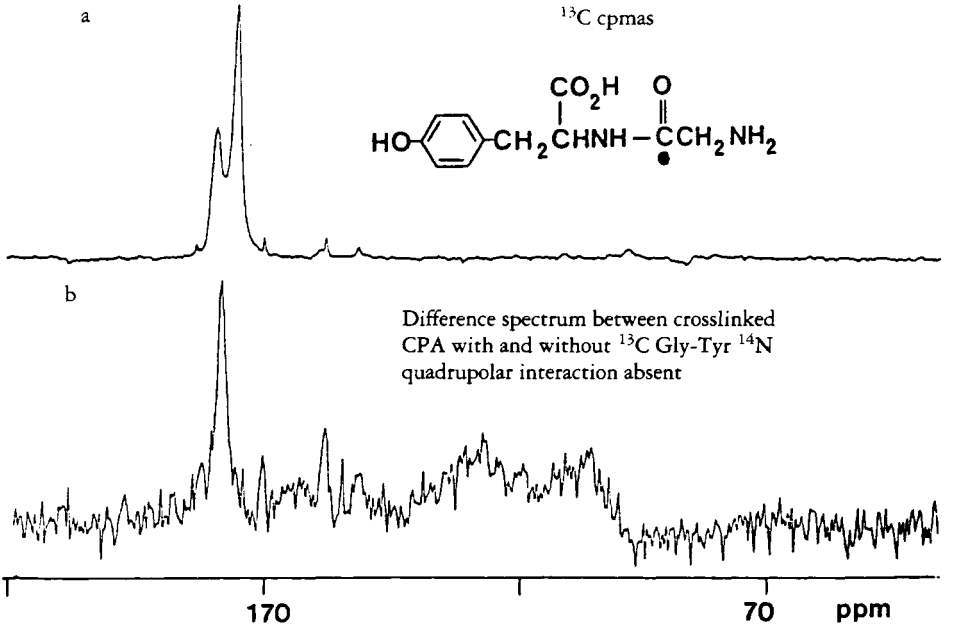

FIGURE 10. 25.15 MHz solid state ^{13}C cpmas spectrum of (a) amido-[^{13}C]Gly-Tyr, ●= ^{13}C, and (b) the difference cpmas spectrum of CPA and CPA/[^{13}C-amido]Gly-Tyr complex. All spectra are 4 K data points with 10 Hz line broadening. (a) Represents 1076 scans and (b) is the weighted difference of 58,027 scans and 50,225 scans.

labeled amido-[^{13}C, ^{15}N]Gly-Tyr (Figure 11a) was bound to CPA under identical conditions and the complex examined by ^{15}N cpmas nmr spectroscopy. As can be seen from Figure 11a, the ^{15}N resonance of the substrate (δ 120 ppm) is sufficiently broad (LW½ 325 Hz) to conceal the ^{15}N-^{13}C one-bond scalar coupling ($J = 16$ Hz). In the enzyme complex (Figure 11c), the observed ^{15}N resonances correspond to the amide region of CPA (see Figure 11b; δ 122 LW½ = 400 Hz) and an amine (69) (δ 42 ppm LW½ = 250 Hz), respectively. We infer from these experiments that we are observing *either* the first stable intermediate of the catalytic pathway, i.e., the anhydride of the cleaved glycine residue bound covalently to Glu-270 (Figure 9b), or the *bound* glycine accompanied in either case by the second product, tyrosine (Figure 11d) also bound to CPA, since in a separate experiment it could be shown that no unbound tyrosine or glycine was present in the complex. A distinction between the two glycine species (anhydride or acid) cannot be made in this experiment because the ^{13}C-chemical shifts of the carbonyl(s) in both the anhydride and the acid are within the observed chemical-shift range. The dis-

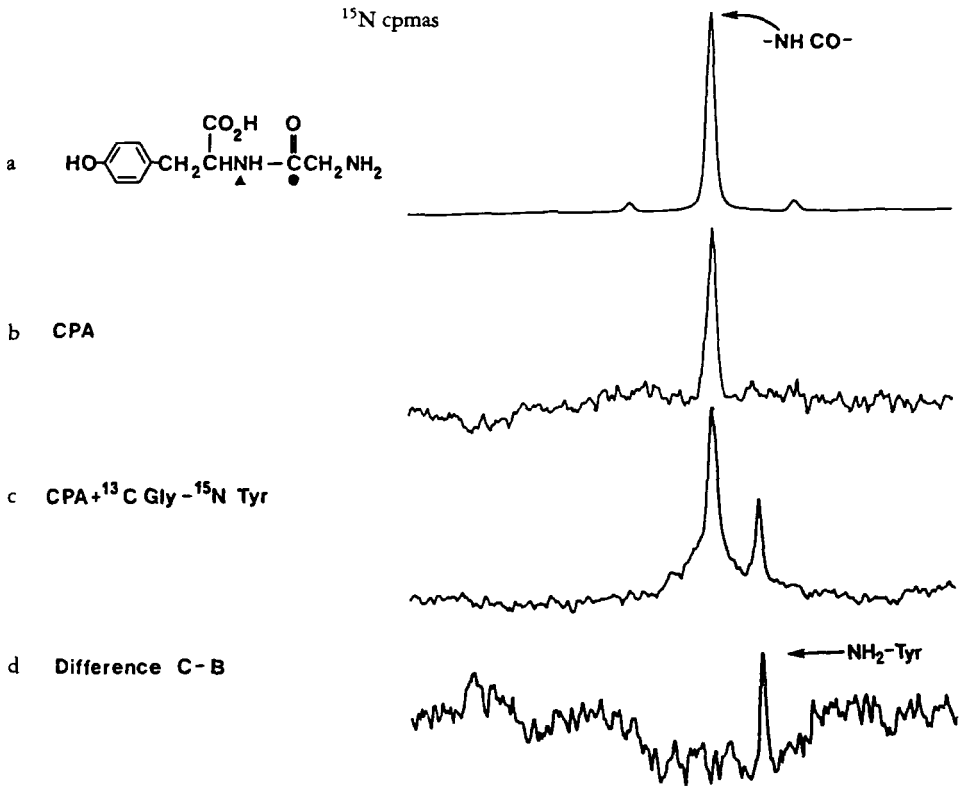

FIGURE 11. 20.28 MHz solid-state ^{15}N cpmas spectrum of (a) amido-[^{13}C,^{15}N]Gly-Tyr, +=^{13}C, ●=^{15}N, (b) CPA, and (c) CPA+amido-[^{13}C,^{15}N]Gly-Tyr. All spectra are 1 K data points with 100 Hz line broadening. (a) Represents 8884 scans, (b) 80,000 scans, while (d) represents the difference between (b) and (c).

tinction is, however, realized by the use of FT-IR difference spectroscopy which indicates that, at least after several days, *no* anhydride (Figure 9b) is present. However, these preliminary experiments clearly indicate the feasibility of simultaneous X-ray and cpmas nmr studies, especially with slow substrates. In summary, a method of some generality for reaching the long-sought correlation between X-ray diffraction data, the resultant geometry of a substrate undergoing slow catalysis, and the corresponding nmr chemical shifts for selected atoms in the *enriched* substrate, obtained under identical conditions, is now available through the use of the cpmas technique, which can be further complemented by FT-IR difference spectroscopy.

From the discussion presented in this section, it is clear that the stage is now set for intensive research into the mechanism of enzyme action with cryoenzymology. Although most of the enzymes discussed above lie in the molecular weight range of 20,000 to 35,000, an upper figure of ~50,000 probably represents the maximum convenient size for ^{13}C-nmr studies on currently available superconducting instruments with substrates and inhibitors.

Finally, we can expect exciting developments in the application of ^{13}C solid-state nmr spectroscopy to structural problems in enzyme complexes, a field which, although still in its infancy, already shows considerable promise (70).

ACKNOWLEDGMENTS

We thank the SERC (U.K.), the National Institutes of Health, and the Robert A. Welch Foundation for generous support at Edinburgh and Texas A&M Universities, and also NATO for providing an exchange program with our colleague Professor G. Müller (Stuttgart).

LITERATURE CITED AND NOTES

1. A.I. Scott, in: *Vitamin B_{12}*. Ed. by B.J. Zagalak and W. Friedrich, Walter de Gruyter & Co., Berlin/New York, 1979, p. 247; A.R. Battersby and E. McDonald, in: *Vitamin B_{12}*. Ed. by D. Dolphin, John Wiley & Sons, New York, 1982, p. 107.
2. K.H. Bergman, R. Deeg, K.D. Gneuss, H.P. Kriemler, and G. Müller, *Z. Physiol. Chem.*, **358**, 1315 (1977); M. Imfeld, D. Arigoni, R. Deeg, and G. Müller, in: *Vitamin B_{12}*. Ed. by B.J. Zagalak and W. Friedrich, Walter de Gruyter & Co., Berlin/New York, 1979, p. 315.
3. A.I. Scott, A.J. Irwin, L.M. Siegel, and J.N. Shoolery, *J. Am. Chem. Soc.*, **100**, 316 and 7987 (1978); A.R. Battersby, E. McDonald, H. Morris, M. Thompson, D.C. Williams, V. Ya. Bykhovsky, N. Zaitseva, and V. Bukin, *Tetrahedron Lett.*, 2217 (1977); A.R. Battersby, E. McDonald, M. Thompson, and V. Ya. Bykhovsky, *J. Chem. Soc. Chem. Commun.*, 150 (1978).
4. (a) G. Müller, K.D. Gneuss, H.P. Kriemler, A.I. Scott, and A.J. Irwin, *J. Am. Chem. Soc.*, **101**, and A.I. Scott, *Tetrahedron* (suppl.), **37**, 81 (1981); (c) A.R. Battersby, G.W.J. Matcham, E. McDonald, R. Neier, M. Thompson, W.D. Woggon, V. Ya. Bykhovsky, and H.R. Morris, *J. Chem. Soc. Chem. Commun.*, 185 (1979); (d) N.G. Lewis, R. Neier, G.W.J. Matcham, E. McDonald, and A.R. Battersby, *J. Chem. Soc. Chem. Commun.*, 541 (1979).
5. Isolation and refeeding experiments have recently shown that sirohydrochlorin (**2**) most probably enters the biochemical pathway at the dihydro level, although reisolated and reincorporated as the fully aromatized macrocycle. See: A.R. Battersby, K. Frobel, F. Hammerschmidt, and C. Jones, *J. Chem. Soc. Chem. Commun.*, 455 (1982).
6. Allusion to these efforts in Cambridge and Texas has been made by A.R. Battersby and by A.I. Scott, see Scott (1) and Uzar and Battersby (16).
7. L. Mombelli, C. Nussbaumer, H. Weber, G. Müller, and D. Arigoni, *Proc. Natl. Acad. Sci. USA*, **78**, 9 (1981).
8. A.R. Battersby, M.J. Bushell, C. Jones, N.G. Lewis, and A. Pfenninger, *Proc. Natl. Acad. Sci. USA*, **78**, 13 (1981).
9. A.I. Scott, C. Yagen, and E. Lee, *J. Am. Chem. Soc.*, **95**, 5761 (1973).
10. G. Müller, in: *Vitamin B_{12}*, Ed. by B.J. Zagalak and W. Friedrich, Walter de Gruyter & Co., Berlin/New York, 1979, p. 279.
11. A.I. Scott, P.B. Reichardt, M.B. Slaytor, and J.G. Sweeny, *Bioorg. Chem.*, **1**, 157 (1971).
12. L. Ernst, *Liebigs Ann. Chem.*, 376 (1981).
13. A.R. Battersby, C. Edington, C.J.R. Fookes, and J.M. Hook, *J. Chem. Soc. (Perkin Trans. 1)*, 2265 (1982).
14. In order to acquire a good signal: noise ratio in the minimum time ($\sim$16 h), a pulse repetition rate of 0.7 sec was used to obtain the spectra shown in Figures 1 and 2. This has the effect of reducing the relative intensities of the C-5 and C-15 methyl signals by about 30-40% due to the long T_1's for C_5 and C_{15} (1.27 and 1.31 sec, respectively). This factor is included in our discussion of the sequence of methylation.
15. M.F. Hegazi, R.T. Borchardt, S. Osaki, and R.L. Schowen, in: *Nucleic Acid Chemistry*, Ed. by L.B. Townsend and R.S. Tipson, John Wiley & Sons, Inc., New York, 1978, p. 889.
16. H.C. Uzar and A.R. Battersby, *J. Chem. Soc. Chem. Commun.*, 1204 (1982).
17. V. Raseetti, A. Pfaltz, C. Kratky, and A. Eschenmoser, *Proc. Natl. Acad. Sci. USA*, **78**, 16 (1981).
18. Based on the concept that cobalt-free corrins exist in nature (19).
19. For alternative mechanisms and a discussion of cobalt insertion, see A.I. Scott, *Pure Appl. Chem.*, **53**, 1215 (1981).
20. T.E. Podschun and G. Müller, *Angew. Chem.*, **97**, 63 (1985).
21. C. Nussbaumer and D. Arigoni, see Eidgenössische Technische Hochschule, Zurich, Diss. #7623.
22. A.I. Scott, N.E. Mackenzie, P.J. Santander, P.E. Fagerness, G. Müller, E. Schneider, R. Sedlmeier, and G. Wörner, *Bioorg. Chem.*, **12**, 356 (1984).
23. G. Burton, P.E. Fagerness, S. Hosozawa, P.M. Jordan, and A.I. Scott, *J. Chem. Soc. Chem. Commun.*, 202 (1979); P.M. Jordan, G. Burton, H. Nordlöv, M.M. Schneider, L. Pryde, and A.I. Scott, *J. Chem. Soc. Chem. Commun.*, 204 (1979).
24. A.R. Battersby, C.J.R. Fookes, G.W.J. Matcham, E. McDonald, and (in part) K.E. Gustafson-Potter, *J. Chem. Soc. Chem. Commun.*, 316 (1979).
25. A.R. Battersby, C.J.R. Fookes, E. McDonald, and G.W.J. Matcham, *Bioorg. Chem.*, **8**, 451 (1979).
26. A.I. Scott, G. Burton, P.M. Jordan, H. Matsumoto, P.E. Fagerness, and L.M. Pryde, *J. Chem. Soc. Chem. Commun.*, 384 (1980).
27. P.M. Anderson and R.J. Desnick, *J. Biol. Chem.*, **255**, 1993 (1980).
28. P.M. Jordan and A. Berry, *Biochem. J.*, **195**, 177 (1981).
29. A. Berry, P.M. Jordan, and J.S. Seehra, *FEBS Lett.*, **129**, 220 (1981).

30. J.N.S. Evans, G. Burton, and A.I. Scott, unpublished results.
31. A.R. Battersby, C.J.R. Fookes, G.W.J. Matcham, E. McDonald, and (in part) R. Hollenstein, *J. Chem. Soc. (Perkin Trans. 1)*, 3031 (1983).
32. A.R. Battersby, C.J.R. Fookes, G. Hart, G.W.J. Matcham, and P.S. Pandey, *J. Chem. Soc. (Perkin Trans. 1)*, 3041 (1983).
33. See Evans (38) for details for the preparative procedures for complex formation.
34. J.A. Elvidge, "Synthesis and Applications of Isotopically Labeled Compounds," in: Proceedings of an International Symposium, Kansas City, MO, June 1982. Ed. by W.P. Duncan and A.B. Susan, Elsevier, Amsterdam, 1983, pp. 35-44 (and references therein).
35. The [^{3}H]PBG employed contains all multiply tritiated species up to the fully tritiated [2,6,6,11,11-$^3H_5$]PBG but consisted mainly of [2-$^3H_1$,6,6-$^3H_2$,11-$^3H_1$]PBG.
36. Prepared by New England Nuclear by custom tritiation according to our directions; see Evans and Scott (37).
37. J.N.S. Evans and A.I. Scott, unpublished results.
38. J.N.S. Evans, Ph.D. Thesis, University of Edinburgh, 1984.
39. One unit is defined as the amount of enzyme required to consume 1 μmol PBG per h.
40. ^{3}H-nmr referencing was performed as follows: A ^{1}H-nmr spectrum of [2,6,6,11,11-$^3H_5$]PBG containing internal $Me_3SiCD_2CD_2CO_2Na$ was recorded and the PBG ^{1}H resonances referenced. The same sample was then examined by ^{3}H nmr in the same probe and referenced to the ^{1}H spectrum ($\delta_{3_H}=\delta_{1_H}$). The absolute field frequency was then used from this to calculate the chemical shifts of subsequent spectra.
41. H. Falk and T. Schlederer, *Monatsh. Chem.*, **112**, 501 (1981). Interestingly, no nmr evidence for the accumulation of HMB (**12a**) was obtained under these conditions involving high concentration (1 mM) of pure deaminase, 3.5°, pH 8.0 [cf. Burton, *et al.* (23), Battersby *et al.* (24,25), and Scott *et al.* (26).
42. R.B. Frydman and G. Feinstein, *Biochim. Biophys. Acta*, **350**, 358 (1974).
43. L. Bogorad, *Plant Physiol.*, **32**, xli (1975).
44. L. Bogorad, in: *Comparative Biochemistry of Photoreactive Systems*. Ed. by M.B. Allen, Academic Press, New York, 1960, p. 227.
45. A.T. Carpenter and J.J. Scott, *Biochim. Biophys. Acta*, **52**, 195 (1968).
46. H. Heath and D.S. Hoare, *Biochem. J.*, **72**, 14 (1959); H. Heath and D.S. Hoare, *Biochem. J.*, **73**, 679 (1959).
47. PBG (**6**) displays a resonance at 4.16 ppm for the C-11 methylene protons and shifts 0.05 ppm upfield on deprotonation (38). The (aminomethyl)bilane (**12** where $CH_2OH=CH_2NH_2$) displays a resonance at 3.92 ppm at pH 12 (48), which implies a methylene chemical shift of 3.97 ppm at pH 8.0.
48. H.O. Dauner, G. Gunzer, I. Heger, and G. Müller, *Hoppe-Seyler's Z. Physiol. Chem.*, **357**, 149 (1976).
49. N.E. MacKenzie, H. Rexhausen, and A.I. Scott (in press). A model thio ether has $\delta=3.3$ ppm for the CH_2-S resonance.
50. P.M. Jordan and D. Shemin, *J. Biol. Chem.*, **248**, 1019 (1973).
51. J.N.S. Evans, P.E. Fagerness, N.E. Mackenzie, and A.I. Scott, *J. Am. Chem. Soc.*, **106**, 5738 (1984).
52. P. Douzou, *Cryobiochemistry*, Academic Press, New York, 1977.
53. T.L. Poulos, R.A. Alden, S.T. Frier, J.J. Burktoft, and J. Kraut, *J. Biol. Chem.*, **251**, 1097 (1976).
54. J.R. Coggins, W. Kray, and E. Shaw, *Biochem. J.*, **138**, 579 (1974).
55. J.P.G. Malthouse, N.E. Mackenzie, A.S.F. Boyd, and A.I. Scott, *J. Am. Chem. Soc.*, **105**, 1685 (1983).
56. A.I. Scott, N.E. Mackenzie, and J.P.G. Malthouse (to be published).
57. J.P.G. Malthouse, M.P. Gamcsik, A.S.F. Boyd, N.E. Mackenzie, and A.I. Scott, *J. Am. Chem. Soc.*, **104**, 6811 (1982).
58. J.P.G. Malthouse and A.I. Scott, *Biochem. J.*, **215**, 555 (1983).
59. N.E. Mackenzie, J.P.G. Malthouse, and A.I. Scott, *Biochem. J.*, **219**, 437 (1984).
60. N.E. Mackenzie, J.P.G. Malthouse, and A.I. Scott, *Science*, **225**, 883 (1984).
61. E.R. Andrew, *Intl. Rev. Phys. Chem.*, **1**, 195 (1981).
62. C.A. Fyfe, J.M. Thomas, J. Klinowski, and G.C. Gobbi, *Angew. Chem., Int. Ed. Engl.*, **22**, 259 (1983).
63. W.N. Lipscomb, J.A. Hartsuck, G.N. Reeke, Jr., F.A. Quiocho, P.H. Bethge, M.L. Ludwig, T.A. Steitz, H. Muirhead and J.C. Coppola, *Brookhaven Symp. Biol.*, **21**, 24 (1968); W.N. Lipscomb, *Acc. Chem. Res.*, **15**, 232 (1982).

64. W.N. Lipscomb, G.N. Reeke, Jr., J.A. Hartsuck, F.A. Quiocho, and P.H. Bethge, *Phil. Trans. Roy. Soc. London, Ser. B*, **257**, 177 (1970).
65. W.N. Lipscomb, in: "Proceedings of The Robert A. Welch Conferences on Chemical Research. XV. Bioorganic Chemistry and Mechanisms," 1971, p. 131; R. Breslow, J. Chin, D. Hilvert and G. Trainor, *Proc. Natl. Acad. Sci. USA*, **80**, 4585 (1983); S.J. Hoffmann, S.S.T. Chu, H. Lee, E.T. Kaiser and P.R. Carey, *J. Am. Chem. Soc.*, **105**, 6971 (1983); L.C. Kuo, J.M. Fukuyama and M.W. Makinen, *J. Mol. Biol.*, **163**, 63 (1982).
66. J.P. Greenstein and M. Winitz, *Chemistry of the Amino Acids*, John Wiley & Sons, Inc., New York, 1961.
67. F.A. Quiocho and F.M. Richards, *Biochemistry*, **5**, 4062 (1966).
68. M.H. Frey and S.J. Opella, *J. Chem. Soc. Chem. Commun.*, 474 (1980).
69. G.C. Levy and R.L. Lichter, *Nitrogen-15 Nuclear Magnetic Resonance Spectroscopy*, John Wiley & Sons, Inc., New York, 1979.
70. N.E. Mackenzie, P.E. Fagerness, and A.I. Scott, *J. Chem. Soc. Chem. Commun.*, 635 (1985).